# Robust Mechanism Discovery with Atom Conserving Chemical Reaction Neural Networks

Felix A. Döppel[1], Martin Votsmeier[1,2,*]

[1] *Technical University of Darmstadt, Peter-Grünberg-Straße 8, 64287 Darmstadt, Germany*
[2] *Umicore AG & Co. KG, Rodenbacher Chaussee 4, 63457 Hanau, Germany*
[*] *martin.votsmeier@tu-darmstadt.de*

**Abstract**

Chemical reaction neural networks (CRNNs) established as the state-of-the-art tool for autonomous mechanism discovery. While they encode some fundamental physical laws, mass- and atom conservation are still violated. We enforce atom conservation by adding a dedicated neural network layer which can be interpreted as constraining the model to physically realizable stoichiometries. Using the standard test cases of the original CRNN paper, we show that the resulting atom conserving chemical reaction neural networks improve training stability and speed, offer robustness against noisy and missing data, and require less data overall. As a result, we anticipate increased model reliability and greater utilization of the potential of real-world data sets. We also discuss the potential of the new atom balance layer for other applications in combustion modeling and beyond, such as mechanism reduction and kinetic surrogate models for reactive flow simulations.

*Keywords:* Atom conservation, Chemical reaction neural networks, Kinetic model, Mechanism discovery, Physics enhanced machine learning

## 1. Introduction

Machine learning has emerged as an important tool in combustion chemistry discovery, reduction and acceleration [1]. The performance of neural networks for these applications is significantly improved by implementing *a priori* physical knowledge in the model's structure. Frequently studied examples in the combustion context are implementing the overall mass or species balances [2, 3]. In this work we focus on implementing the atom balance in neural networks. Previously, this has either been done explicitly through a soft constraint in the loss function [4, 5], or a post-processing step [6], or indirectly by embedding the stoichiometric matrix into the model's structure [7–10]. However, in case of mechanism discovery and reduction, the stoichiometric matrix is generally unknown and subject to optimization. We propose a dedicated element balance layer for neural networks models of chemical kinetics that enforces atom conservation as a hard constraint without requiring the stoichiometric matrix. We implement this layer into the chemical reaction neural network (CRNN) recently developed by JI and DENG [11], and demonstrate that enforcing the atom conservation greatly increases the model's ability to identify reaction mechanisms from low quality data.

The CRNN is a digital twin of the classic chemical reaction network that encodes the Arrhenius equation (Eq. 1) and the mass-action law (Eq. 2) in a neural network

$$k_j = A_0 \cdot T^{\beta} \cdot \exp\left(\frac{-E_A}{R \cdot T}\right) \tag{1}$$

$$r_j = k_j \cdot \prod_i a_i^{\nu_{i,j}} \tag{2}$$

with the rate constant $k_j$ of reaction $j$, the pre-exponential $A_0$, the temperature $T$, the temperature exponent $\beta$, the activation energy $E_A$, the universal gas constant $R$, the reaction rate $r_j$, the activity $a_i$ of species $i$ and the reaction orders $\nu_{i,j}$.

BARWEY and RAMAN used such a digital twin to accelerate chemical source term evaluations of large combustion mechanisms to facilitate high-fidelity simulations of turbulent flames [12]. The main advantage of the CRNN, however, is the ability to autonomously discover and reduce mechanisms using readily available integral reactor measurements with the neural ordinary differential equation (neural ODE) technique [13]. JI and DENG used this approach to obtain reaction mechanisms from several chemical and biochemical engineering systems [11]. It has further been applied to biomass pyrolysis [3], decomposition of energetic materials [14–16], hydrogen as well as methane combustion [17], and *HyChem* models [18].

The current CRNN implementation infringes the fundamental law of atom conservation. We enforce this law through our atom balance layer, building on the original CRNN implementation. The resulting atom conserving chemical reaction neural networks (AC-CRNN) increase training stability and speed, provide robustness against noisy and missing data, and reduce the overall amount of data required. This is an important step to learn from imperfect data as they are typically obtained from experiments.

For simplicity, we will consider the standard example systems from JI and DENG [11]. We showcase the superior AC-CRNN performance under the influence of three realistic imperfect data scenarios: 1. limited data availability, 2. noisy data and 3. systematic measurement errors.

## 2. Atom Conserving Chemical Reaction Neural Networks

Conventional CRNNs find the stoichiometric coefficients of a reaction mechanism by freely optimizing the weights of their output layer. However, not all combinations of stoichiometric coefficients satisfy the fundamental law of atom conservation. A physically realizable set of stoichiometric coefficients $\nu_i$ fulfills the equation

$$0 = \sum_i N_{k,i} \cdot \nu_i \tag{3}$$

with the molecular matrix $\mathbf{N}$ that contains the number of atoms of type $k$ per species $i$ [19]. In other words: All physically realizable vectors $\nu$ are in the null space of $\mathbf{N}$. A basis $\mathbf{B}$ of this null space is conveniently computed by the MATLAB function `null` or the Julia function `LinearAlgebra.nullspace` which are based on singular value decomposition. Now all valid sets of stoichiometric coefficients can be expressed as a weighted sum of the basis vectors

$$\nu = \mathbf{B} \cdot w. \tag{4}$$

A neural network that learns the weights $w$ and multiplies them with the basis $\mathbf{B}$ to obtain stoichiometric coefficients will always fulfill atom conservation. We implement Eq. 4 by adding a dedicated element balance layer to the CRNN (Fig 1) and call the resulting architecture *atom conserving chemical reaction neural networks* (AC-CRNN). The matrix $\mathbf{B}$ has $N_{\text{key}} = N_{\text{species}} - \text{rank}(\mathbf{N})$ columns, which is fewer than the total number of species present in the reaction system $N_{\text{species}}$ [20]. Therefore, the element balance layer does not only enforce atom conservation but also reduces the number of trainable parameters. In our AC-CRNN, the stoichiometric coefficients are further used to derive the reaction orders of the reactants using the ReLu function

$$\text{ReLu}(x) = \max(x, 0) \tag{5}$$

To further increase the interpretability of the AC-CRNN, we propose to apply the concept of key species by converting the null space basis matrix $\mathbf{B}$ into reduced column echelon form. This means that the first $N_{\text{key}}$ rows contain a identity matrix. The matrix conversion can be conveniently achieved using

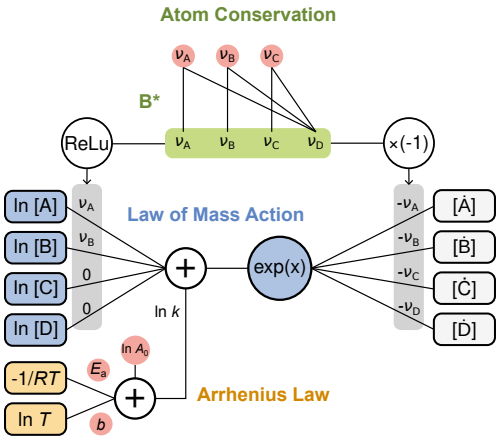


Fig. 1: Schematic representation of an AC-CRNN reaction node. It encodes the law of mass action, the Arrhenius law and in contrast to the original CRNN also the atom conservation. Latter is achieved by multiplication of the key species coefficients with the conservation matrix $\mathbf{B}^*$. Multiple such reaction nodes are combined in a single hidden layer to build up a chemical reaction neural network. Trainable parameters are highlighted in red.

the `rref` function in MATLAB or the Julia library *RowEchelon.jl*. We call this basis the atom conservation matrix $\mathbf{B}^*$. For test case 1,

$$\mathbf{B}^* = \begin{bmatrix} 1 & 0 & 0 & 0 \\ 0 & 1 & 0 & 0 \\ 0 & 0 & 1 & 0 \\ 0 & 0 & 0 & 1 \\ -1/3 & -2/3 & -1/3 & -1/3 \end{bmatrix} \tag{6}$$

Here, the first $N_{\text{key}}$ weights $w$ are directly mapped to the first $N_{\text{key}}$ stoichiometric coefficients. We call those species whose coefficients are identical to the learned weights $w$ the key species. Which species are treated as key species can be chosen by the user through the order of the species in the vector $\nu$. Always the first $N_{\text{key}}$ species are treated as key species. The coefficients of the other species are a weighted sum of the key species coefficients.

Altogether, implementing the element balance layer adds a minimum amount of additional code to the original CRNN. The matrix B* is computed in a fully automated preprocessing step. The code for this step is supplied in the appendix. Due to the reduced number of trainable parameters and the regularization provided by the additional physical constraints, AC-CRNNs generally train faster than the corresponding CRNN. All results presented in this work are obtained using the basis $\mathbf{B}^*$. It has been found, that the AC-CRNN that uses $\mathbf{B}^*$ shows better performance than the one using the unconverted basis $\mathbf{B}$. Further, the performance depends on the choice of the key species.

## 3. Methods

In practice, species concentrations at certain positions of the reactor are measured instead of source terms. Therefore, the CRNN is trained in the context of a neural ODE [13], i.e. wrapped with an ODE solver. The resulting CRNN concentration profiles $c^{\text{CRNN}}(t)$ are compared to the provided concentration data $c^{\text{data}}(t)$. We use the Julia language implementation of CRNN available at `https://github.com/DENG-MIT/CRNN`. It uses the differential programming package *DifferentialEquations.jl* [21] to enable backpropagation of gradients through the ODE solver. The mean absolute error MAE loss (Eq. 7) of the normalized concentrations (Eq. 8) is used and minimized using the ADAM optimizer [22] to adjust the CRNN parameters.

$$\text{loss} = \text{MAE}\left(c^{\text{CRNN}}_{\text{norm}}(t), c^{\text{data}}_{\text{norm}}(t)\right) \tag{7}$$

$$c_{\text{norm}} = \frac{c(t)}{\text{range}(c^{\text{data}}(t))} \tag{8}$$

In test case 1 the initial CRNN parameters are randomly drawn from a standard normal distribution and divided by 1000. The ADAM algorithm is used for 15 000 epochs with a learning rate of 0.001, an exponential decay for the first (0.9) and second (0.999) momentum estimate and a weight decay of $10^{-8}$. In test case 2 the initial CRNN parameters are randomly drawn from a normal distribution and divided by 10, for $\ln A_0$ and activation energies 0.8 is added and absolute values are used for activation energies. The ADAM algorithm is used for 10 000 epochs with a learning rate of 0.005, an exponential decay for the first (0.9) and second (0.999) momentum estimate and a weight decay of $10^{-6}$.

## 4. Results and Discussion

We demonstrate, that embedding the atom balance into neural networks facilitates mechanism discovery. Test case 1 is a demonstration system considering mass conservation to reduce the required amount of training data. Test case 2 is a realistic example of biodiesel production kinetics where embedding the atom balance increases the model's robustness against noise and offsets in the training data. Finally, we discuss further applications in surrogate modeling and mechanism reduction.

### *4.1. Test Case 1 - Trimerization*

Test case 1 is a representative example for mechanism discovery introduced by SEARSON *et al.* [23] and describes the trimerization of a generic molecule A. This could for example be the formation of benzene from ethyne or the homotrimerization of proteins, such as porins [24] or hemagglutinin [25]. The reaction system consists of five species called A, $A_2$, $A^*$, $A^{**}$, and $A_3$ that are involved in four reactions:

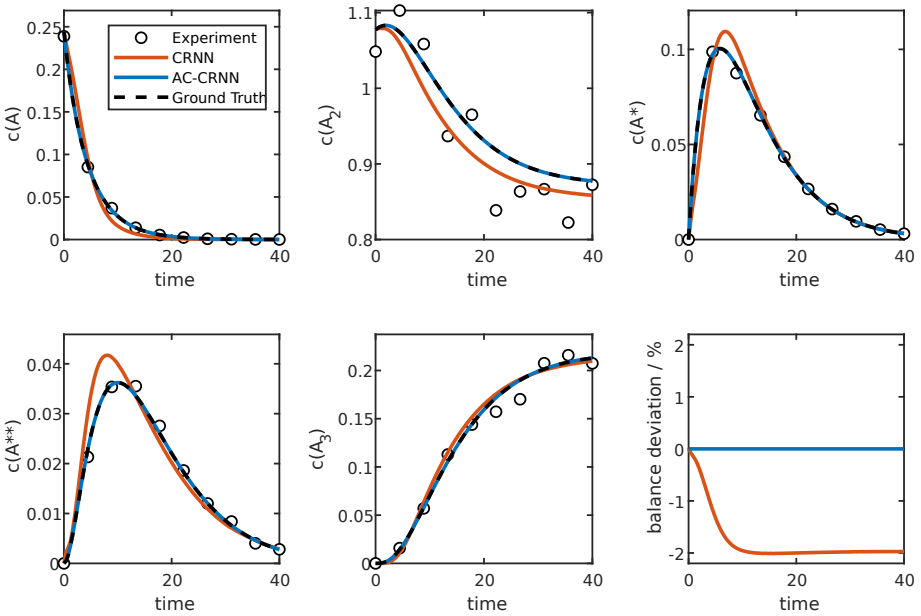


Fig. 2: Predicted concentration profiles obtained by fitting standard CRNN and atom conserving CRNN (AC-CRNN) to 20 synthetic integral reactor experiments with 10 noisy concentration measurements each are compared with the reference model (groud truth). The CRNN overestimates the consumption of species B and looses about 2% of the total mass. The AC-CRNN is biased towards a physically plausible solution by the embedded element balance and therefore hardly distinguishable from the exact solution.

$$2\,\mathrm{A} \xrightarrow{\mathrm{k_1}} \mathrm{A_2}$$
$$\mathrm{A} \xrightarrow{\mathrm{k_2}} \mathrm{A^*}$$
$$\mathrm{A^*} \xrightarrow{\mathrm{k_3}} \mathrm{A^{**}}$$
$$\mathrm{A_2} + \mathrm{A^{**}} \xrightarrow{\mathrm{k_4}} \mathrm{A_3}$$

The rate constants $k_1 - k_4$ are not temperature dependent and are assumed to have the values 0.3, 0.1, 0.2, and 0.13 respectively. Initial concentrations of species A and $A_2$ are randomly chosen with uniform distribution between 0.2 and 1.2, the other species are not present in the initial mixture. Experimental concentration measurements are emulated by integrating this initial value problem with the Tsitouras 5/4 Runge-Kutta method [21] up to a reaction time of 40 s, sampling data at equidistant time intervals and adding 5% gaussian noise.

JI and DENG showed that CRNNs are able to recover the mechanism from 20 of those simulated isothermal experiments with 100 data points each [11]. We test the CRNN performance for even fewer data (10 points per experiment), increasing the problem difficulty significantly. To tackle this problem, we introduce atom conserving CRNN (AC-CRNN) that embed the atom conservation matrix $\mathbf{B}^*$ into the CRNN (Fig. 1). The conservation matrix is obtained as the reduced column echelon form of the null space basis of the molecular matrix (Tab. 1) using the MATLAB functions `null` and `rref`.

Table 1: The molecular matrix shows the composition of the species of the trimerization case.

| | A |
|---|---|
| A | 1 |
| $A_2$ | 2 |
| $A^*$ | 1 |
| $A^{**}$ | 1 |
| $A_3$ | 3 |

In this example, the rank of the molecular matrix is one, so there will be one dependent species and four key species. Without loss of generality, we choose species $A_3$ as the dependent species. The resulting atom conservation matrix (Eq. 6) is used to calculate the stoichiometric coefficient of $A_3$ as a weighted sum of the coefficients of the other four species. This guarantees atom conservation and reduces the number of trainable parameters.

Figure 2 shows that the original CRNN models tends to overestimate the formation of the intermediate species. Resulting inconsistencies in the stoichiometric matrix of the model lead to a violation of atom conservation. The AC-CRNN, however, is

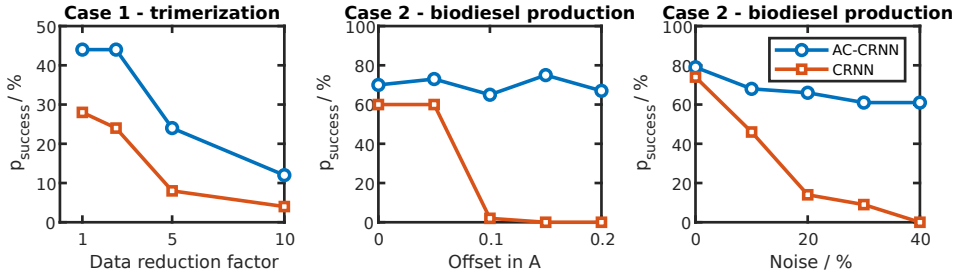


Fig. 3: Fraction of successful mechanism discovery attempts $p_{\text{success}}$ of atom conserving AC-CRNN compared to standard CRNN in various scenarios of realistic data flaws. Due to the additional physical bias (here, atom conservation), AC-CRNN are much more robust against left: reduced data availability middle: systematic measurement errors and right: lower data quality.

forced to obey atom conservation and therefore much more likely to identify the correct mechanism. For example, AC-CRNN solutions that overestimate the formation of intermediate species automatically underestimate other species and are therefore penalized with a higher loss.

To further characterize the performance of the networks, we discuss the success probability $p_{\text{success}}$ of the training, see Saerson et al. [23]. It is defined as the fraction of successful mechanism discovery attempts from different initial model states. Here, we consider a mechanism discovery attempt successful, if every estimated stoichiometric coefficient differs by less than 0.1 from the ground truth. The success probability of the original CRNN drops from 25% using 100 data points to 4% using only 10 data points per experiment (Fig. 3). Enforcing atom conservation increases the success probability to 44% and 12% respectively.

### *4.2. Test Case 2 - Biodiesel Production*

Test case 2 considers biodiesel production, as studied by BURNHAM *et al.* [26]. DARNOKO and CHERYAN [27] described the transesterification of palm oil derived palmitin glycerides (TG, DG, and MG) with methanol MeOH to smaller methyl esters $RCO_2Me$ by three consecutive reactions:

$$\mathrm{TG} + \mathrm{MeOH} \xrightarrow{\mathrm{k_1}} \mathrm{DG} + \mathrm{RCO_2Me}$$

$$\mathrm{DG} + \mathrm{MeOH} \xrightarrow{\mathrm{k_2}} \mathrm{MG} + \mathrm{RCO_2Me}$$

$$\mathrm{MG} + \mathrm{MeOH} \xrightarrow{\mathrm{k_3}} \mathrm{GL} + \mathrm{RCO_2Me}$$

The temperature dependence of the rate constants is described by the arrhenius equation with the preexponentials $A_0$ (18.60, 19.13, and 7.93), the activation energies $E_A$ (14.54, 14.42, and 6.47) kcal/mol and a temperature exponent of 0 for all three reactions. The Tsitouras 5/4 Runge-Kutta method with automatic switching to an order 2/3 L-Stable Rosenbrock method [21] is used to integrate the potentially stiff initial value problem.

A CRNN is used to identify reaction orders, stoichiometric coefficients, activation energies and the preexponential factors. For this, 20 experiments with random initial concentrations between 0.2 and 2.2 arbitrary units at temperatures randomly chosen between 323 K to 343 K are provided. Each experiment consists of 50 noisy (5% gaussian noise) concentration measurements taken after a time step of 1 seconds each. Collecting such an amount of precise measurements is experimentally very challenging, so after we showed with test case 1 that AC-CRNN provide accurate results even with small amounts of data, we now test the robustness against systematic measurement errors in the provided training data in form of a sensor offset that overestimates the concentrations of species TG by 0.2.

Table 2: The molecular matrix shows the elemental composition of the species of the biodiesel production case.

| | C | H | O |
|---|---|---|---|
| TG | 51 | 98 | 6 |
| MeOH | 1 | 4 | 1 |
| DG | 35 | 68 | 5 |
| MG | 19 | 38 | 4 |
| GL | 3 | 8 | 3 |
| $RCO_2Me$ | 17 | 34 | 2 |

The system contains six species and can be balanced in terms of the three elements carbon, hydrogen and oxygen (Tab. 2). Without loss of generality we choose methanol, the di- and the triglyceride as key species. The stoichiometric coefficients of the other three species are inferred from the key species coefficients using the atom conservation matrix

$$B^* = \begin{bmatrix} 1 & 0 & 0 \\ 0 & 1 & 0 \\ 0 & 0 & 1 \\ -3 & 1 & -2 \\ 2 & -1 & 1 \\ 0 & -1 & 0 \end{bmatrix} \tag{9}$$

where the rows correspond to all species (TG, MeOH, DG, MG, GL, and $RCO_2Me$) and the columns correspond to the key species (TG, MeOH, and DG). Bal-

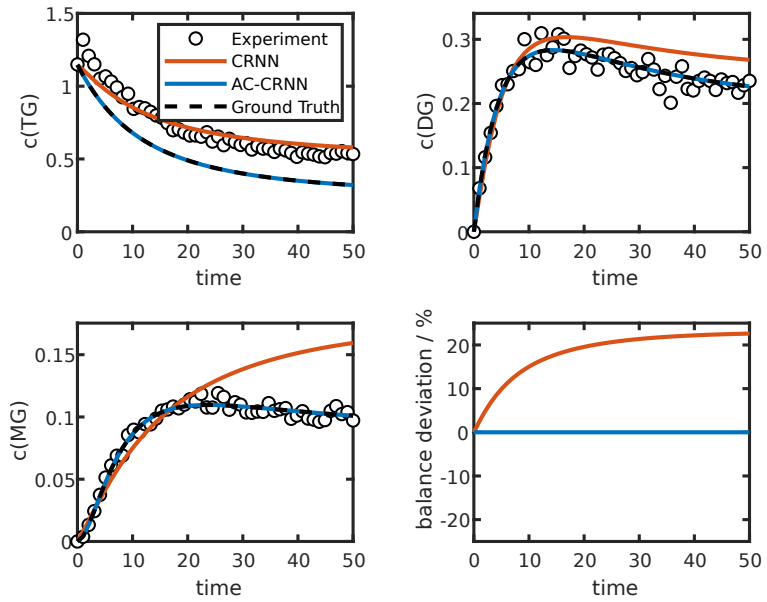


Fig. 4: Biodiesel production concentration profiles obtained from mechanism discovery by standard CRNN and atom conserving CRNN (AC-CRNN) using synthetic measurements from 20 integral reactor experiments. To mimic realistic concentration measurements the data given for model training ("Experiment") are perturbed by 5% gaussian noise. The triglyceride data are additionally shifted by an offset of 0.2. As the CRNN adapts to the artificially high concentrations in the reactant (TG), too much of the glyceride products (DG and MG) is formed, resulting in a significant deviation from the element balance. The AC-CRNN is constrained by the embedded element balance and therefore not affected by the sensor offset.

ancing in terms of molecular groups such as glycerol, acid rest, and methyl rest would lead to the same conservation matrix.

Figure 4 shows a typical CRNN prediction in case of a sensor offset. As the model adapts to the erroneously high concentrations of the reactant TG, an excessive amount of the other glycerides DG and MG is formed. This leads to an error in the atom balance by more than 20%. The AC-CRNN has 37.5% fewer parameters to optimize and trains correspondingly faster. Further, it is stable towards the sensor offset (Fig. 4) and shows a perfectly closed atom balance. It successfully recovers the correct mechanism in 70% of the runs, whereas the original CRNN is not successful in any out of 60 runs. Similarly, increasing the amount of gaussian noise applied to the concentration measurements from 5% to 40%, the success probability of the standard CRNN drops to 0%, while the AC-CRNN is remains successful in 60% of the runs (Fig. 3). Here, mechanism discovery is considered successful, if every estimated stoichiometric coefficient differs by less than 0.2 from the ground truth.

### *4.3. Applications of the atom balance layer beyond CRNNs*

Because the proposed atom balance layer can be combined with any feed forward neural network that predicts kinetics, it should find widespread use in combustion and beyond, for example in surrogate modeling and mechanism reduction.

Aside from CRNN, our element balance layer should be useful in conjunction with other network structures that discover reaction mechanisms and thus lack an a priori stoichiometric matrix. One example is the PolyODEnet by Wu *et al.* [28].

The proposed key species approach can be applied intuitively to small reaction systems without explicitly using the matrix $\mathbf{B}^*$. This is a common way to achieve atom conservation in surrogate models of catalytic systems [29–33]. Our element balance layer formalizes this approach, allowing its application to more complex systems.

Finally, our approach is easily extended to also implement the charge balance relevant for redox- and electrochemical reactions.

## 5. Conclusion

Chemical reaction neural networks (CRNN) have established as the most advanced tool for autonomous mechanism discovery and are used in many fields, such as (bio-) chemical engineering, pyrolysis, and combustion. While they encode the law of mass action as well as the Arrhenius law, mass- and atom conservation are still violated.

We enforce the fundamental law of atom conservation by adding a dedicated neural network layer

which can be interpreted as constraining stoichiometric coefficients to physically realizable combinations. The resulting atom conserving chemical reaction neural networks (AC-CRNN) improve training stability and speed, offer robustness against noisy and missing data, and require less data overall. As a result, we anticipate increased model reliability and greater utilization of the potential of real-world data sets. Our proposed element conservation layer is compatible with any feed forward neural network that predicts kinetics and should therefore be useful also for surrogate modeling and mechanism reduction.

## Declaration of competing interest

The authors declare that they have no known competing financial interests or personal relationships that could have appeared to influence the work reported in this paper.

## Acknowledgments

This work was funded by BMBF in the framework of the project ML-MORE (contract 05M20RDA). The authors gratefully acknowledge the computing time provided on the high-performance computer Lichtenberg at the NHR Centers NHR4CES at TU Darmstadt.

## Appendix

The generation of the atom conservation matrix $\mathbf{B}^*$ from the molecular matrix $\mathbf{N}$ is demonstrated using the following MATLAB code using the example of test case 1:

```
N = [1,2,1,1,3]';
B_star = rref(null(N')')'
```

## References

[1] T. Echekki, A. Farooq, M. Ihme, S. M. Sarathy, Machine Learning for Combustion Chemistry, Springer International Publishing, Cham, 2023, pp. 117–147. doi:10.1007/978-3-031-16248-0_5.

[2] A. J. Sharma, R. F. Johnson, D. A. Kessler, A. Moses, Deep Learning for Scalable Chemical Kinetics, in: AIAA Scitech 2020 Forum, Vol. 1 PartF, American Institute of Aeronautics and Astronautics, Reston, Virginia, 2020. doi:10.2514/6.2020-0181.

[3] W. Ji, F. Richter, M. J. Gollner, S. Deng, Autonomous kinetic modeling of biomass pyrolysis using chemical reaction neural networks, Combustion and Flame 240 (2022) 111992. arXiv:2105.11397, doi:10.1016/j.combustflame.2022.111992.

[4] C. Chi, X. Xu, D. Thévenin, Efficient premixed turbulent combustion simulations using flamelet manifold neural networks: A priori and a posteriori assessment, Combustion and Flame 245 (August) (2022) 112325. doi:10.1016/j.combustflame.2022.112325.

[5] A. Almeldein, N. Van Dam, Accelerating Chemical Kinetics Calculations With Physics Informed Neural Networks, Journal of Engineering for Gas Turbines and Power 145 (9) (2023) 1–14. doi:10.1115/1.4062654.

[6] K. Wan, C. Barnaud, L. Vervisch, P. Domingo, Machine learning for detailed chemistry reduction in DNS of a syngas turbulent oxy-flame with side-wall effects, Proceedings of the Combustion Institute 38 (2) (2021) 2825–2833. doi:10.1016/j.proci.2020.06.047.

[7] P. O. Sturm, A. S. Wexler, Conservation laws in a neural network architecture: enforcing the atom balance of a Julia-based photochemical model (v0.2.0), Geoscientific Model Development 15 (8) (2022) 3417–3431. doi:10.5194/gmd-15-3417-2022.

[8] T. Kircher, F. A. Döppel, M. Votsmeier, A neural network with embedded stoichiometry and thermodynamics for learning kinetics from reactor data (2023) 1–35doi:10.26434/chemrxiv-2023-rpr35.

[9] A. Fedorov, A. Perechodjuk, D. Linke, Kinetics-Constrained Neural Ordinary Differential Equations: Artificial Neural Network Models tailored for Small Data to boost Kinetic Model Development (2023) 1–25doi:10.26434/chemrxiv-2023-x39xt.

[10] F. Sorourifar, Y. Peng, I. Castillo, L. Bui, J. Venegas, J. A. Paulson, Physics-Enhanced Neural Ordinary Differential Equations: Application to Industrial Chemical Reaction Systems, Industrial & Engineering Chemistry Research 62 (38) (2023) 15563–15577. doi:10.1021/acs.iecr.3c01471.

[11] W. Ji, S. Deng, Autonomous Discovery of Unknown Reaction Pathways from Data by Chemical Reaction Neural Network, Journal of Physical Chemistry A 125 (4) (2021) 1082–1092. arXiv:2002.09062, doi:10.1021/acs.jpca.0c09316.

[12] S. Barwey, V. Raman, A Neural Network-Inspired Matrix Formulation of Chemical Kinetics for Acceleration on GPUs, Energies 14 (9) (2021) 2710. doi:10.3390/en14092710.

[13] R. T. Q. Chen, Y. Rubanova, J. Bettencourt, D. Duvenaud, Neural Ordinary Differential Equations (jun 2018). arXiv:1806.07366.

[14] H. Wang, Y. Xu, M. Wen, W. Wang, Q. Chu, S. Yan, S. Xu, D. Chen, Kinetic modeling of CL-20 decomposition by a chemical reaction neural network, Journal of Analytical and Applied Pyrolysis 169 (November 2022) (2023) 105860. doi:10.1016/j.jaap.2023.105860.

[15] G. Tang, H. Wang, C. Chen, Y. Xu, D. Chen, D. Wang, Y. Luo, X. Li, Thermal decomposition of nano Al-based energetic composites with fluorinated energetic polyurethane binders: experimental and theoretical understandings for enhanced combustion and energetic performance, RSC Advances 12 (37) (2022) 24163–24171. doi:10.1039/d2ra03781e.

[16] Y. Xu, Q. Chu, X. Chang, H. Wang, S. Wang, S. Xu, D. Chen, Thermal decomposition mechanism of 1,3,5-trinitroperhydro-1,3,5-triazine: Experiments and reaction kinetic modeling, Chemical Engineering Science 282 (June) (2023) 119234. doi:10.1016/j.ces.2023.119234.

[17] J. Huang, Y. Zhou, W. A. Yong, Data-driven discovery of multiscale chemical reactions governed by the law of mass action, Journal of Computational Physics 448 (2022) 110743. arXiv:2101.06589, doi:10.1016/j.jcp.2021.110743.

[18] W. Ji, J. Zanders, J.-W. Park, S. Deng, Machine Learning Approaches to Learn HyChem Models (2021). arXiv:2104.07875.

[19] D. R. Schneider, G. Reklaitis, On material balances for chemically reacting systems, Chemical Engineer-

ing Science 30 (2) (1975) 243–247. doi:10.1016/0009-2509(75)80012-1.
[20] M. Baerns, A. Behr, H. Hofmann, J. Gmehling, U. Onken, A. Renken, K.-O. Hinrichsen, R. Palkovits, Technische chemie, John Wiley & Sons, 2013.
[21] C. Rackauckas, Q. Nie, DifferentialEquations.jl – A Performant and Feature-Rich Ecosystem for Solving Differential Equations in Julia, Journal of Open Research Software 5 (1) (2017) 15. doi:10.5334/jors.151.
[22] D. P. Kingma, J. Ba, Adam: A method for stochastic optimization, arXiv preprint arXiv:1412.6980 (2014).
[23] D. P. Searson, M. J. Willis, A. Wright, Reverse Engineering Chemical Reaction Networks from Time Series Data, Statistical Modelling of Molecular Descriptors in QSAR/QSPR 2 (2012) 327–348. doi:10.1002/9783527645121.ch12.
[24] S. Galdiero, A. Falanga, M. Cantisani, R. Tarallo, M. Elena Della Pepa, V. D'Oriano, M. Galdiero, Microbe-Host Interactions: Structure and Role of Gram-Negative Bacterial Porins, Current Protein and Peptide Science 13 (8) (2012) 843–854. doi:10.2174/138920312804871120.
[25] C. S. Copeland, R. W. Doms, E. M. Bolzau, R. G. Webster, A. Helenius, Assembly of influenza hemagglutinin trimers and its role in intracellular transport., The Journal of cell biology 103 (4) (1986) 1179–1191. doi:10.1083/jcb.103.4.1179.
[26] S. C. Burnham, D. P. Searson, M. J. Willis, A. R. Wright, Inference of chemical reaction networks, Chemical Engineering Science 63 (4) (2008) 862–873. doi:10.1016/j.ces.2007.10.010.
[27] D. Darnoko, M. Cheryan, Kinetics of palm oil transesterification in a batch reactor, JAOCS, Journal of the American Oil Chemists' Society 77 (12) (2000) 1263–1267. doi:10.1007/s11746-000-0198-y.
[28] Q. Wu, T. Avanesian, X. Qu, H. Van Dam, PolyODENet: Deriving mass-action rate equations from incomplete transient kinetics data, Journal of Chemical Physics 157 (16) (2022). doi:10.1063/5.0110313.
[29] M. Votsmeier, Efficient implementation of detailed surface chemistry into reactor models using mapped rate data, Chemical Engineering Science 64 (7) (2009) 1384–1389. doi:10.1016/j.ces.2008.12.006.
[30] F. A. Döppel, M. Votsmeier, Efficient machine learning based surrogate models for surface kinetics by approximating the rates of the rate-determining steps, Chemical Engineering Science 262 (2022) 117964. doi:10.1016/j.ces.2022.117964.
[31] F. A. Döppel, M. Votsmeier, Efficient neural network models of chemical kinetics using a latent asinh rate transformation, Reaction Chemistry & Engineering 8 (10) (2023) 2620–2631. doi:10.1039/D3RE00212H.
[32] F. A. Döppel, T. Wenzel, R. Herkert, B. Haasdonk, M. Votsmeier, Goal-Oriented Two-Layered Kernel Models as Automated Surrogates for Surface Kinetics in Reactor Simulations, Chemie Ingenieur Technik (2023). doi:10.1002/cite.202300178.
[33] B. Klumpers, T. Luijten, S. Gerritse, E. Hensen, I. Filot, Direct coupling of microkinetic and reactor models using neural networks, Chemical Engineering Journal (2023) 145538doi:10.1016/j.cej.2023.145538.